Beyond leading-order logarithmic scaling in the catastrophic self-focusing of a laser beam in Kerr media

Pavel M. Lushnikov,* Sergey A. Dyachenko, and Natalia Vladimirova
Department of Mathematics and Statistics, University of New Mexico, Albuquerque, New Mexico 87131, USA
(Received 5 August 2012; revised manuscript received 18 February 2013; published 29 July 2013)

We study the catastrophic stationary self-focusing (collapse) of a laser beam in nonlinear Kerr media. The width of self-similar solutions near the collapse distance $z = z_c$ obeys the $(z_c - z)^{1/2}$ scaling law with the well-known leading-order modification of loglog type $\propto (\ln|\ln(z_c - z)|)^{-1/2}$. We show that the validity of the loglog modification requires double-exponentially large amplitudes of the solution $\sim 10^{10^{100}}$, which is unrealistic to achieve in either physical experiments or numerical simulations. We derive an equation for the adiabatically slow parameter which determines the system self-focusing across a large range of solution amplitudes. Based on this equation we develop a perturbation theory for scaling modifications beyond the leading loglog. We show that, for the initial pulse with the optical power moderately above ($\lesssim 1.2$) the critical power of self-focusing, the scaling agrees with numerical simulations beginning with amplitudes around only three times above the initial pulse.

DOI: 10.1103/PhysRevA.88.013845 PACS number(s): 42.65.Jx, 52.38.Hb

I. INTRODUCTION AND THE MAIN RESULT

The catastrophic collapse (self-focusing) of a high-power laser beam has been routinely observed in nonlinear Kerr media since the advent of lasers [1–4]. The propagation of a laser beam through the Kerr media is described by the nonlinear Schrödinger equation (NLSE) in dimensionless form,

$$i\partial_z\psi + \nabla^2\psi + |\psi|^2\psi = 0, \tag{1}$$

where the beam is directed along the z axis, $\mathbf{r} \equiv (x,y)$ are the transverse coordinates, $\psi(\mathbf{r},z)$ is the envelope of the electric field, and $\nabla \equiv (\frac{\partial}{\partial x}, \frac{\partial}{\partial y})$. NLSE (1) also describes the dynamics of attractive Bose-Einstein condensate (BEC) [5] (z is replaced by the time variable in that case). In addition, the NLSE emerges in numerous optical, hydrodynamic, and plasma problems and describes the propagation of nonlinear waves in general nonlinear systems with cubic nonlinearity.

If only one transverse coordinate is taken into account, then the NLSE is integrable by the inverse scattering transform [6] leading to global existence of all solutions (solutions exist for all z). A solution of the NLSE which depends on both transverse coordinates (x,y) can develop a singularity ("blowup") such that the amplitude of the solution reaches infinity in a finite distance z_c. Since the blowup is accompanied by dramatic contraction of the spatial extent of function ψ, it is called "wave collapse" or simply "collapse" [7,8]. Near the singularity $z = z_c$, the NLSE loses applicability, and either dissipative or nondissipative effects must be taken into account. Such effects can include the optical damage and formation of plasma in the Kerr media, inelastic scattering in the BEC, or plasma density depletion in high-temperature laser-plasma interactions [9,10].

Equation (1) can be rewritten in the Hamiltonian form

$$i\psi_t = \frac{\delta H}{\delta \psi^*}, \tag{2}$$

with the Hamiltonian

$$H = \int \left(|\nabla\psi|^2 - \frac{1}{2}|\psi|^4\right) d\mathbf{r}. \tag{3}$$

Another conserved quantity, $N \equiv \int |\psi|^2 d\mathbf{r}$, has the meaning of the optical power (or the number of particles in the BEC). The sufficient condition for the collapse is $H < 0$, while the necessary condition is $N > N_c$, where N_c is the critical power defined below.

While the large power $N \gg N_c$ typically produces multiple collapses (multiple filamentation of the laser beam [11]) with strong turbulence behavior [12,13], the dynamics of each collapsing filament is universal and can be considered independently. Each collapsing filament carries the power N only moderately above N_c. We consider a single collapsing filament (laser beam) centered at $\mathbf{r} = 0$. For $z \to z_c$ the collapsing solution of the NLSE quickly approaches the cylindrically symmetric solution, which is convenient to represent through the following change of variables [4]:

$$\psi(r,z) = \frac{1}{L}V(\rho,\tau)e^{i\tau + iLL_z\rho^2/4}, \quad |\mathbf{r}| \equiv r, \quad L_z \equiv \frac{dL}{dz}. \tag{4}$$

Here, $L(z)$ is the z-dependent beam width,

$$\rho = \frac{r}{L} \quad \text{and} \quad \tau = \int_0^z \frac{dz'}{L^2(z')} \tag{5}$$

are blowup variables such that $\tau \to \infty$ as $z \to z_c$. Transformation (4) was inspired by the discovery of the additional conformal symmetry of the NLSE which is called the "lens transform" [14–16].

It follows from Eqs (1), (4), and (5) that $V(\rho,\tau)$ satisfies

$$i\partial_\tau V + \nabla_\rho^2 V - V + |V|^2 V + \frac{\beta}{4}\rho^2 V = 0, \tag{6}$$

where

$$\beta = -L^3 L_{zz}, \quad L_{zz} \equiv \frac{d^2L}{dz^2}, \quad \text{and} \quad \nabla_\rho^2 \equiv \partial_\rho^2 + \rho^{-1}\partial_\rho. \tag{7}$$

As $z \to z_c$, β approaches zero adiabatically slowly and $V(\rho)$ approaches the ground-state soliton $R(\rho)$ [16]. The ground-

*plushnik@math.unm.edu

state soliton is the radially symmetric, z-independent solution of the NLSE, $-R + \nabla_\rho^2 R + R^3 = 0$. It is positive definite, i.e., $R > 0$, with asymptotic $R(\rho) = e^{-\rho}[A_R \rho^{-1/2} + O(\rho^{-3/2})]$, with $\rho \to \infty$ and $A_R \equiv 3.518\,062\ldots$ [16]. Also R defines the critical power

$$N_c \equiv 2\pi \int R^2 \rho d\rho = 11.700\,896\,5\ldots. \tag{8}$$

The limiting behavior in $V \to R$ as $z \to z_c$ implies that the $\partial_\tau V$ term in Eq. (6) is a small correction compared to the other terms. Also β can be interpreted as a quantity proportional to the excess of particles above critical, $N - N_c$, in the collapsing region [16,17].

References [18,19] found that the leading-order dependence of $L(z)$ has the following square-root-loglog form:

$$L \simeq \left(2\pi \frac{z_c - z}{\ln|\ln(z_c - z)|}\right)^{1/2}. \tag{9}$$

(Reference [18] has a "slip of pen" in a final expression, see, e.g., Ref. [20] for a discussion.) The validity of the scaling (9) at $z \to z_c$ was rigorously proven in Ref. [21]. However, numerous attempts to verify the modification of $L \propto (z_c - z)^{1/2}$ scaling have failed to give convincing evidence of the loglog dependence (see, e.g., Refs. [22,23]). The lack of validity of the loglog law was also discussed in Ref. [16]. Note that without logarithmic modification, the scaling $(z_c - z)^{1/2}$ implies $\beta = \text{const}$, $N = \infty$, and infinitely fast rotation of the phase for $r \to \infty$ with $\beta \neq 0$. Thus, the logarithmic modification is necessary and is responsible for the adiabatically slow approach of β to 0.

A qualitatively similar problem of logarithmic modification of square-root scaling also occurs in the Keller-Segel equation, which describes either the collapse of self-gravitating Brownian particles or the chemotactic aggregation of microorganisms [24–28]. It was shown in Refs. [28,29] that the leading logarithmic modification in the Keller-Segel equation is valid only for very large amplitudes ($\gtrsim 10^{10000}$). Also in Refs. [28,29], the perturbation theory was developed beyond the leading-order logarithmic correction. That theory was shown to be accurate starting from moderate amplitudes ($\gtrsim 3$) of the collapsing solution.

Following qualitatively some ideas of Refs. [28,29], in this paper we develop the perturbation theory about the self-similar solution of Eq. (6) with $V \simeq R(\rho)$ and show that the scaling (9) dominates only for very large amplitudes,

$$|\psi| \gtrsim 10^{10^{100}}. \tag{10}$$

Instead of pursuing this unrealistic limit, we suggest the following expression (derived below) as a practical choice for the experimental and theoretical study of self-focusing:

$$\begin{aligned}
L &= [2\pi(z_c - z)]^{1/2}\left(\ln A - 4\ln 3 + 4\ln\ln A + \frac{4(-1 - 4\ln 3 + 4\ln\ln A)}{\ln A}\right.\\
&\quad \left. + \frac{-28 - 80\ln 3 - 32(\ln 3)^2 - \pi^2 c_1 + 80\ln\ln A + 64(\ln 3)\ln\ln A - 32[\ln\ln A]^2}{(\ln A)^2}\right)^{-1/2},\\
A &= -3^4 \frac{\tilde{M}}{2\pi^3}\ln\left[[2\pi(z_c - z)]^{1/2}\frac{e^{-b_0}}{L(z_0)}\right], \quad \tilde{M} = 44.773\ldots, \quad \beta_0 = \beta(z_0), \quad c_1 = 4.743\ldots, \quad c_2 = 52.37\ldots,\\
b_0 &= \frac{e^{\frac{\pi}{\sqrt{\beta_0}}}}{\tilde{M}}\left(\frac{2\beta_0^2}{\pi} + \frac{8\beta_0^{5/2}}{\pi^2} + \frac{2\beta_0^3(20 + \pi^2 c_1)}{\pi^3} + \frac{12\beta_0^{7/2}(20\pi^3 + \pi^5 c_1)}{\pi^7} + \frac{2\beta_0^4(840\pi^3 + 42\pi^5 c_1 + \pi^7 c_2)}{\pi^8}\right).
\end{aligned} \tag{11}$$

This expression depends on an additional parameter, z_0, defined below. Also A and b_0 are introduced to provide a more compact form of the expression (11). $L(z)$ is only weakly sensitive to the choice of $z_0 < z_c$ provided z_0 is larger than the smallest distance at which the collapsing solution has approximately reached the self-similar form.

To illustrate the poor agreement with the loglog law at moderate amplitudes, Fig. 1 shows the dynamics of $L(z)$ obtained from numerical simulations. The simulations were started with different initial conditions in the form of Gaussian beams $\psi(\mathbf{r},0) = pe^{-r^2}$ with the power $N = \pi p^2/2$. Figure 1 shows that $L(z)$ neither agrees with the loglog law (9) nor is it universal. In contrast, the dependence of β_τ on β appears to be universal as demonstrated in Fig. 2. The curves corresponding to different initial conditions converge to a single $\beta_\tau(\beta)$ curve after the initial transient evolution. The resulting single curve is universal and independent of initial conditions. This universality is the key for the analytical theory developed below. Note that the dependence of β on $z - z_c$ is also not universal as seen in Fig. 3, so it cannot be used effectively for the development of the analytical theory.

Figure 1 also demonstrates the excellent agreement between the analytical expression (11) and numerical simulations of the NLSE (1). Figure 4 shows the relative error between $L(z)$ obtained from the numerical simulations of the NLSE (1) and $L(z)$ from Eq. (11). The relative errors decreases with the decrease of $(N - N_c)/N_c$. The only exception is the curve for a significantly larger power, $N/N_c = 1.208$, which is formally beyond the applicability of Eq. (11). Equation (11) is derived in the limit $(N - N_c)/N_c \to 0$, as explained below. However, even in the case of $N/N_c = 1.208$ the relative error $\lesssim 6\%$. In evaluating Eq. (11) we used the parameters $L_0 = L(z_0)$ and $\beta_0 = \beta(z_0)$ taken from numerical simulations at locations $z = z_0$. These locations are shown by the thick dots in Fig. 1. Similarly, the thick dots show the corresponding points $\beta(z_0)$ and $\beta_\tau(z_0)$ in Figs. 2 and 3. We choose z_0 as the propagation

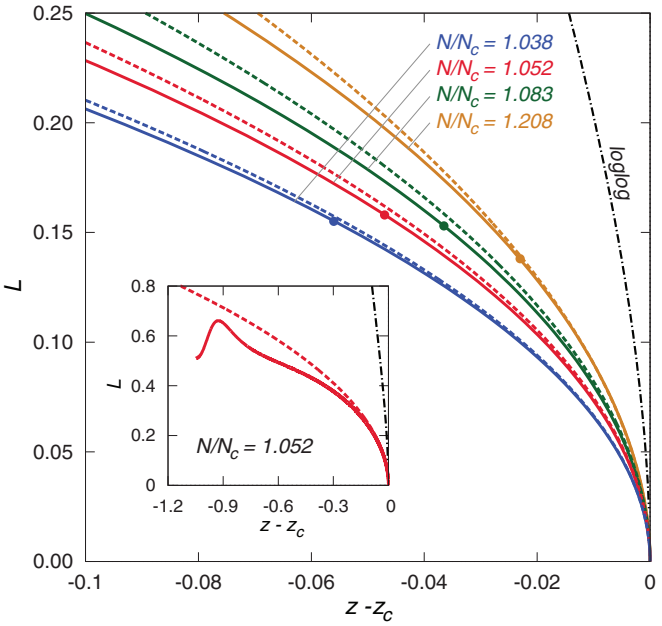

FIG. 1. (Color online) A dependence of the beam width L on $z - z_c$ obtained from numerical simulations of the NLSE (1) (solid lines) and from Eq. (11) (dashed lines) for different initial conditions. Each pair of closely spaced solid and dashed lines corresponds to the same Gaussian initial condition $\psi(r,0) = pe^{-r^2}$. The curves are labeled by the power $N = \pi p^2/2$ (scaled by the critical power N_c). The dash-dotted line shows L from the loglog law (9). The dashed lines are obtained from Eq. (11) using the parameters $L_0 = L(z_0)$ and $\beta_0 = \beta(z_0)$ taken from numerical simulations at locations $z = z_0$. These locations are marked by the thick dots on each solid line. These values of z_0 are chosen by the criterion $[\max_{\mathbf{r}} |\psi(\mathbf{r},z_0)|]/[\max_{\mathbf{r}} |\psi(\mathbf{r},0)|] = 5$. The inset shows $L(z)$ for $N/N_c = 1.052$ starting from the beginning of the simulation, $z = 0$. It is seen in the inset that about a twofold decrease of L compared with the initial value $L(0)$ already produces a good agreement between the simulation of the NLSE (1) and Eq. (11). All units here and in subsequent figures are dimensionless.

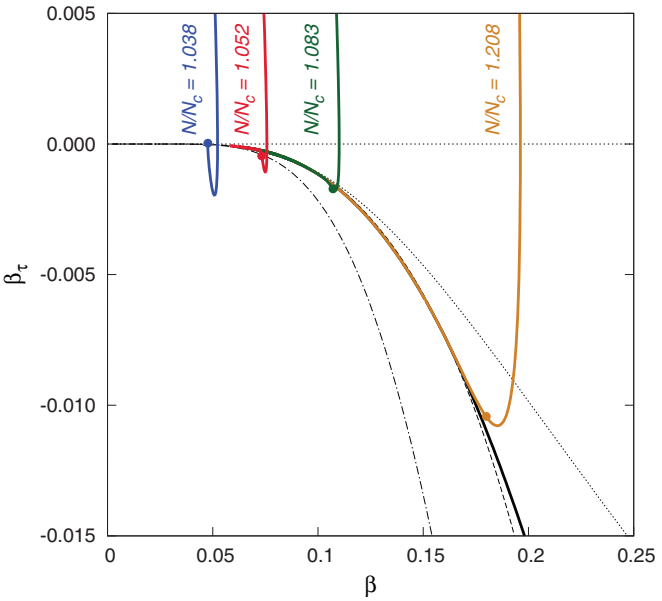

FIG. 2. (Color online) Lines show $\beta_\tau(\beta)$ from numerical simulations of the NLSE (1) with the same initial conditions as in Fig. 1. The curves are labeled by the values of N/N_c. It is seen that the solid curves converge to a single universal $\beta_\tau(\beta)$ curve after the initial transient evolution. The universal curve is independent of the initial conditions. Similar to Fig. 1, the thick dots mark the locations of $z = z_0$ at each solid line; i.e., they indicate the pairs of points $[\beta(z_0),\beta_\tau(z_0)]$. The dashed line corresponds to $\beta_\tau(\beta)$ from Eq. (16). See also the text for the description of the dash-dotted and dotted lines.

distance where the amplitude of the collapse exceeds the initial amplitude of the Gaussian pulse by a factor of 5, i.e., $[\max_{\mathbf{r}} |\psi(\mathbf{r},z_0)|]/[\max_{\mathbf{r}} |\psi(\mathbf{r},0)|] = 5$. Choosing z_0 larger than defined above (e.g., by a tenfold increase of the collapse amplitude) results only in very small variations ($\lesssim$0.2%) of dashed lines in Fig. 1 for $N/N_c \lesssim 1.1$. It means that the prediction of analytical expression is only weakly dependent on z_0.

The paper is organized as follows. In Sec- II we approximate the collapsing solution by the expansion about the soliton solution in blowup variables. The perturbations of this solution determines the rate of collapse which allows us to derive the reduced ordinary differential equation (ODE) system for the unknowns $L(z)$ and $\beta(z)$. In Sec. III we find the asymptotic solution of this reduced system in the limit $z \to z_c$ and derive the scaling (11). In Sec. IV we estimate the range of applicability of a NLSE collapsing solution in experiment. In Sec. V we briefly describe the method used in the NLSE simulation, and we discuss the procedure for the extraction of the parameters of the collapsing solutions $\beta(z)$ and $L(z)$ from the simulations. In Sec. VI the main results of the paper are discussed.

II. REDUCTION OF NLSE COLLAPSING SOLUTION TO ODE SYSTEM FOR $L(z)$ AND $\beta(z)$

To determine $\beta_\tau(\beta)$ analytically, we consider the ground-state soliton solution $V_0(\beta,\rho)$ of Eq. (6) given by

$$\nabla_\rho^2 V_0 - V_0 + V_0^3 + \frac{\beta}{4}\rho^2 V_0 = 0. \tag{12}$$

The function $V_0(\beta,\rho)$ has an oscillating tail, $V_0(\beta,\rho) = c\rho^{-1}\cos[\frac{\beta^{1/2}}{4}\rho^2 - \beta^{-1/2}\ln\rho + \phi_0] + O(\rho^{-3})$, with $c,\phi_0 =$ const and $\rho \gg 2/\beta^{1/2}$. Here, by ground-state soliton V_0, we mean the real function such that it minimizes $|c|$ in the tail. It implies that V_0 has only small amplitude oscillations with $|c| \ll 1$ for $0 < \beta \ll 1$.

The full solution $V(\beta,\rho)$ of Eq. (6) is well approximated by $V_0(\beta,\rho)$ for $\rho \lesssim 1$. However, the small but nonzero value of $\partial_\tau V_0 = \beta_\tau \frac{dV_0}{d\beta}$ provides an imaginary contribution to V. To account for the imaginary contribution at the leading order, we allow V_0 to be complex (replacing it by $\tilde{V}_0$), similar to the approach of Refs. [12,16]. We formally add an exponentially small term $i\nu(\beta)\tilde{V}_0$ to Eq. (12) as follows, $\nabla^2\tilde{V}_0 - \tilde{V}_0 + |\tilde{V}_0|^2\tilde{V}_0 + \frac{\beta}{4}\rho^2\tilde{V}_0 - i\nu(\beta)\tilde{V}_0 = 0$. The yet unknown $\nu(\beta)$ accounts for the loss of power of $\tilde{V}_0$ by emission into the tail. One can reinterpret the resulting

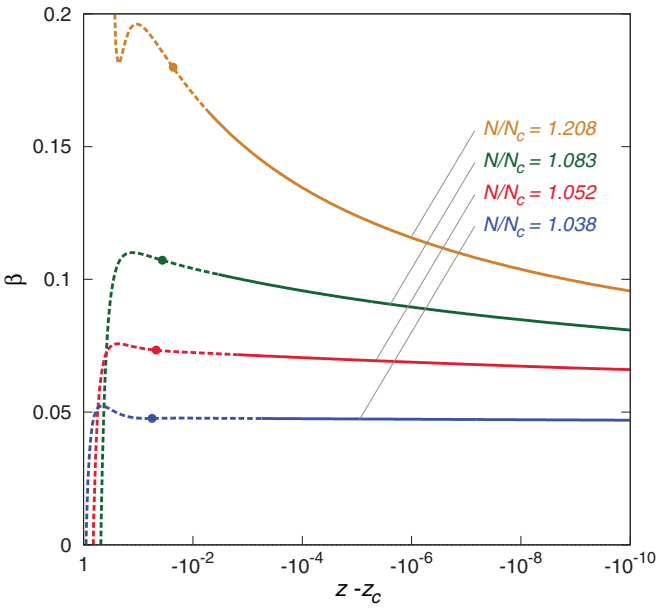

FIG. 3. (Color online) Dependence of β on $z - z_c$ for the same set of simulations as in Fig. 1. The initial fast evolution is responsible for the formation of the quadratic phase [see Eq. (4)] and is specific to our Gaussian initial conditions with zero phase. The evolution slows down after β passes through the local maximum; the following change in β is especially slow for smaller values of N/N_c. The transitions from dashed to solid lines indicate the collapse of the corresponding $\beta_\tau(\beta)$ curves onto the single universal curve shown in Fig. 2. The relative difference of 10^{-3} between a particular simulation curve and the universal curve is used as a transition criterium. Similar to Fig. 1, the thick dots mark the locations of $z = z_0$.

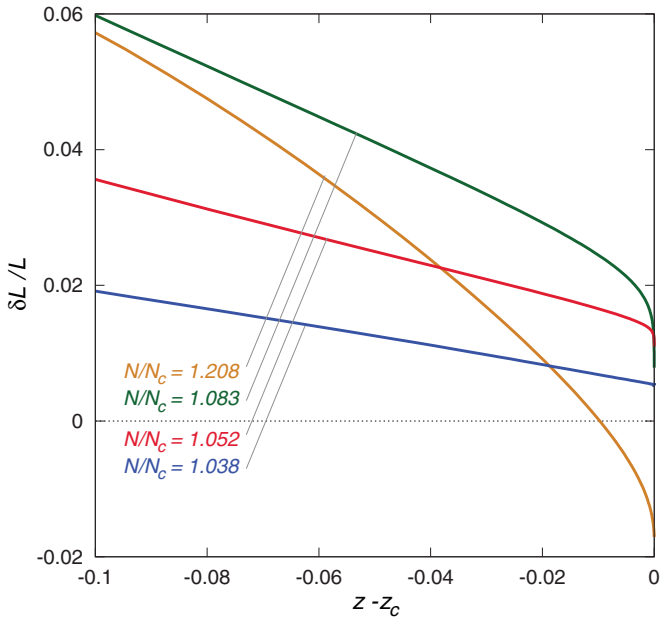

FIG. 4. (Color online) The relative error, $\delta L/L$, between $L(z)$ obtained from the numerical simulations of the NLSE (1) and $L(z)$ from Eq. (11) for the same set of simulations as in Fig. 1. It is seen that the relative errors decreases as $(N - N_c)/N_c$ approaches zero. The exception is the curve for the much larger value $N/N_c = 1.208$, where Eq. (11) is formally on the boundary of its range of applicability.

equation as a linear Schrödinger equation with a self-consistent potential $U \equiv -|\tilde{V}_0|^2 - \frac{\beta}{4}\rho^2$ and a complex eigenvalue $E \equiv -1 - i\nu(\beta)$. (This type of non-self-adjoint boundary value problem was introduced by Gamov in 1928 in the theory of α decay [30].) Assuming $\beta \ll 1$, we identify two turning points, $\rho_a \sim 1$ and $\rho_b \simeq 2/\beta^{1/2}$, at which $\mathrm{Re}E + U = 0$. Using the WKB (Wentzel-Kramers-Brillouin) approximation we consider the tunneling from the collapsing region $\rho \lesssim 1$ through the classically forbidden region $\rho_a < \rho < \rho_b$ and obtain, similar to Ref. [12], that

$$\tilde{V}_0 = e^{-\frac{\pi}{2\beta^{1/2}}} \exp\left[i\frac{\beta^{1/2}}{4}\rho^2 - i\beta^{-1/2}\ln\rho - i\tilde{\phi}_0\right] \times \frac{2^{1/2}A_R}{\beta^{1/4}}[\rho^{-1} + O(\rho^{-3})], \quad \tilde{\phi}_0 = \text{const}, \quad \rho \gg \rho_b, \tag{13}$$

where A_R results from the matching of the asymptotic of R with the WKB solution. We also note that the tail (13) is derived in the adiabatic approximation which is valid for large but finite values of the radius, $2/\beta^{1/2} \ll r/L \ll A\,(2/\beta^{1/2})$, where $A(z) \gg 1$ is a slowly changing factor in comparison with $L(z)$. Even though for $r/L \gtrsim A\,(2/\beta^{1/2})$ the solution is not self-similar [20,31,32], its large-radius asymptotic has no influence on $L(z)$ and is not considered here.

We define the power (the number of particles) N_b in the collapsing region $\rho < \rho_b$ as

$$N_b = \int_{r<\rho_b L} |\psi|^2 d\mathbf{r} = 2\pi \int_{\rho<\rho_b} |V|^2 \rho d\rho \tag{14}$$

and a flux P beyond the second turning point $\rho_b = 2/\sqrt{\beta}$ as $P = 2\pi\rho[iVV_\rho^* + \text{c.c.}]|_{\rho=\rho_b}$, where c.c. stands for complex conjugate terms. From conservation of N, the flux P determines the change of N_b as

$$\frac{dN_b}{d\tau} = -2\pi\rho[iVV_\rho^* + \text{c.c.}], \quad \rho \gg \rho_b, \tag{15}$$

where we approximated P at $\rho = \rho_b$ through its value at $\rho \gg \rho_b$, taking advantage of almost constant flux to the right of the second turning point. Using the adiabatic assumption that $\frac{dN_b}{d\tau} = \beta_\tau \frac{dN_b}{d\beta}$, and approximating V in Eq. (15) by Eq. (13), we obtain that

$$\beta_\tau = -4\pi A_R^2 \left(\frac{dN_b}{d\beta}\right)^{-1} e^{-\frac{\pi}{\beta^{1/2}}}. \tag{16}$$

Recalling the definition of $\nu(\beta)$, one can also find $\nu(\beta) \simeq (2\pi A_R^2/N_b)e^{-\frac{\pi}{\beta^{1/2}}}$ from Eq. (16).

The next step is to find $\frac{dN_b}{d\beta}$ in Eq. (16). We base our derivation on a crucial observation that the absolute value $|V(\beta,\rho)|$ of the numerical solution of Eq. (6) coincides with $V_0(\beta,\rho)$ for $0 \leqslant \rho \lesssim \rho_b$, as shown in Fig. 5. The approximation $V_0(\beta,\rho) \simeq R(\rho) + dV(\beta,\rho)/d\beta|_{\beta=0}$ used previously (see, e.g., Ref. [16]) is limited to $\rho \ll \rho_b$ because the amplitude c of the tail of V_0 has the essential complex singularity $c \propto e^{-\pi/(2\beta^{1/2})}$ for $\beta \to 0$. Approximating N_b through replacing V in Eq. (14) by

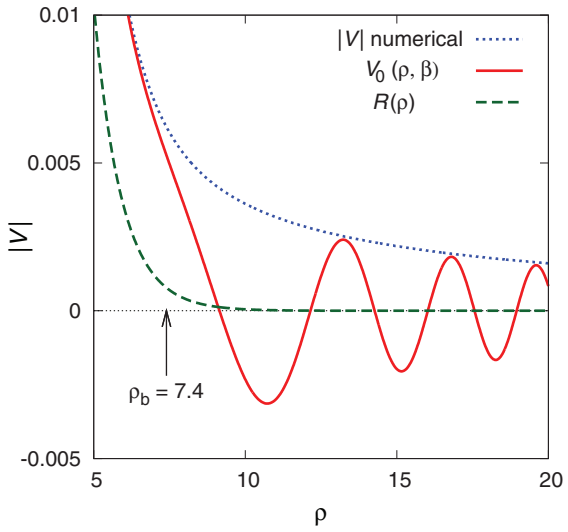

FIG. 5. (Color online) Asymptotic $\rho \gg 1$ for V_0 (solid line), full numerical solution $|V|$ (dotted line), and R (dashed line) for $\beta = 0.073$. It is seen that V_0 and $|V|$ almost coincide for $\rho < \rho_b$.

$V_0(\beta,\rho)$ we obtain the following series:

$$\frac{dN_b}{d\beta} = 2\pi M[1 + c_1\beta + c_2\beta^2 + c_3\beta^3 + c_4\beta^4 + c_5\beta^5], \quad (17)$$

where $M \equiv (2\pi)^{-1} dN_b/d\beta|_{\beta=0} = (1/4)\int_0^\infty \rho^3 R^2(\rho) d\rho = 0.552\,858\,97\ldots$ and coefficients $c_1 = 4.742\,80$, $c_2 = 52.3697$, $c_3 = 297.436$, $c_4 = -4668.01$, and $c_5 = 10566.2$ are estimated from the numerical solution of Eq. (12). Here the value of c_1 is obtained from the numerical differentiation: $c_1 = (2\pi M)^{-1} d^2N_b/d\beta^2|_{\beta=0}$. One can in principle find coefficients $c_2, c_3, \ldots$ from higher-order numerical differentiation at $\beta = 0$. However, the radius of convergence of the corresponding Taylor series is $\beta \sim 0.04$. Yet the range of β resolved in our NLSE simulations is $\beta \gtrsim 0.05$ as seen in Fig. 2. Thus it would be inefficient to use the Taylor series (centered at $\beta = 0$) to approximate $\frac{dN_b}{d\beta}$ in Eq. (17) for $\beta \gtrsim 0.05$. Instead we approximate $c_2, \ldots, c_5$ from the polynomial fit in the range $0.0 < \beta < 0.23$. This procedure gives the numerical values given above. The relative error between the exact value of $\frac{dN_b}{d\beta}$ and the polynomial interpolation (17) is $<1.6\%$ in the range $0 \leqslant \beta < 0.23$. If only c_1 and c_2 are taken into account in Eq. (17), then the relative error is $< 1.0\%$ in the range $0 \leqslant \beta < 0.09$. Figure 2 shows that Eqs. (16) and (17) approximate well the full numerical solution for $\beta \lesssim 0.18$. Indeed, $\beta_\tau(\beta)$ from Eq. (16) with $dN_b/d\beta$, obtained either numerically via $V_0(\beta,\rho)$ or by using Eq. (17), are indistinguishable on the plot (they are both shown by the dashed line). The dotted line corresponds to Eq. (17) with only c_1 and c_2 taken into account.

For comparison, the dash-dotted line in Fig. 2 shows the standard approximation for $\beta_\tau(\beta)$ [16], which corresponds to Eq. (17) with the expression in square brackets replaced by 1. As we see, the standard approximation fails all way down to $\beta \approx 0.05$. Further decrease of β is unresolvable in our simulations (which typically reach $\max|\psi| \sim 10^{15}$).

From Eqs. (5), (7), (16), and (17) we obtain a closed system:

$$\frac{d\beta}{d\tau} = -\frac{2A_R^2}{M(1 + c_1\beta + c_2\beta^2 + c_3\beta^3 + c_4\beta^4 + c_5\beta^5)} \times e^{-\frac{\pi}{\beta^{1/2}}}, \quad (18a)$$

$$\frac{d^2L}{dz^2} = -L^{-3}\beta, \quad (18b)$$

$$\frac{d\tau}{dz} = L^{-2}, \quad (18c)$$

from which the unknowns $\beta(z)$ and $L(z)$ can be determined. This system is the ODE system for independent variable z because τ can be easily excluded from the system using Eq. (18c).

III. ASYMPTOTIC SOLUTION OF THE REDUCED SYSTEM

In this section we look for the asymptotic solution of the reduced system (18), in the limit $z \to z_c$, $\tau \to \infty$, $\beta \to 0$, and $L \to 0$ to derive our main result, Eq. (11). We introduce the adiabatically slow variable

$$a = -L\frac{dL}{dz}, \quad (19)$$

which is also expressed through τ as $a = -L^{-1}\frac{dL}{d\tau}$ according to Eq. (18c). Here and below, we use the same notations for all functions with the same physical meaning, independently of their arguments: $L = L(z) = L(\tau) = L(\beta)$, etc.

Using Eqs. (18c) and (19) we obtain that

$$\beta = a^2 + a_\tau. \quad (20)$$

However, the adiabatic slowness of a requires $a_\tau \ll a^2$ because, by the chain rule of differentiation, $a_\tau = a_\beta\beta_\tau$ while β_τ is exponentially small for $\beta \ll 1$, as follows from Eq. (18a). Then at the leading order we obtain from Eq. (20) that

$$a = \beta^{1/2}. \quad (21)$$

Using Eq. (19) we obtain that $dz = -\beta^{-1/2} L dL$, which allows us to explicitly integrate Eq. (18a) in terms of variables L and β and their initial values $L_0 = L(z_0)$, $\beta_0(z_0)$ (z_0 is defined above). The explicit expression is cumbersome and includes the exponential integral function $Ei(\pi/\beta^{1/2})$, $Ei(x) = -\int_{-x}^{\infty} e^{-y} y^{-1} dy$. We asymptotically expand this expression for $\pi/\beta^{1/2} \gg 1$ to obtain the following expression:

$$-\ln\frac{L}{L_0} = \frac{2\pi^3 e^x}{\tilde{M}}\left[\frac{1}{x^4} + \frac{4}{x^5} + \frac{20 + \pi^2 c_1}{x^6} + \frac{120 + 6\pi^2 c_1}{x^7} + \frac{840 + 42\pi^2 c_1 + \pi^4 c_2}{x^8} + O\left(\frac{1}{x^9}\right)\right]\Bigg|_{x=\pi/\beta_0^{1/2}}^{x},$$

$$x \equiv \frac{\pi}{\beta^{1/2}}, \quad \tilde{M} = \frac{2A_R^2}{M}. \quad (22)$$

The addition of the correction term a_τ in Eq. (20) can be easily done as a small perturbation. For the range of parameters considered in our simulations, such a correction would result in the change of all the solutions by $<1\%$. Therefore the correction is omitted in this paper. Deriving Eq. (11), we used

leading-order terms with only c_1 and c_2 taken into account in Eq. (17). [The corresponding $\beta_\tau(\beta)$ is shown by a dotted line in Fig. 2.] Thus c_1 and c_2 in Eq. (17) are sufficient to produce very good agreement with the simulations shown in Fig. 1.

When Eq. (22) is interpreted as an implicit expression for x as a function of $\ln \frac{L}{L_0}$, it becomes a remote relative of the Lambert W function. Such an implicit expression can be solved for x assuming $x \gg 1$ by iterations as follows:

$$x = L_1 + 4L_2 - 4\ln 3 + \frac{4(4L_2 - 1 - 4\ln 3)}{L_1} + \frac{16\big[-2L_2^2 + L_2(5 + 4\ln 3) - 2(\ln 3)^2 - 5\ln 3\big]}{L_1^2} + \frac{-28 - \pi^2 c_1}{L_1^2} + O\left(\frac{L_2^3}{L_1^3}\right), \tag{23}$$

where

$$L_1 = \ln\left[\frac{3^4\tilde{M}}{2\pi^3}\left(\ln\frac{L_0}{L} + b_0\right)\right], \quad L_2 = \ln L_1, \tag{24}$$

with b_0 defined in Eq. (11) [b_0 is proportional to the right-hand side of Eq. (22) with $x = \pi/\beta_0^{1/2}$]. The factor 3^4 in the definition of L_1 is somewhat arbitrary: we can multiply both sides of Eq. (22) by the arbitrary constant before starting the interation procedure to derive Eq. (23). This factor shows up in Eq. (23) through terms with powers of $\ln 3$. The particular choice of 3^4 allows us to speed up the convergence of the series expansion (23) for not very large values of L_1.

We now introduce the collapse distance z_c into the system (18) as follows

$$z_c - z = \int_z^{z_c} dz' = -\int_L^0 \frac{L'dL'}{a(L')} = \int_{-\infty}^{\ln L} \frac{(L')^2 d\ln L'}{[\beta(L')]^{1/2}}, \tag{25}$$

where we used Eqs. (19) and (21). Using Eq. (23) we express β in Eq. (25) through L. Then we evaluate the integral in Eq. (25) asymptotically for $\ln L \to -\infty$ using the Laplace method (see, e.g., Refs. [33,34]) which gives

$$z_c - z = \frac{L^2}{2\pi}\left[L_1 - 4\ln 3 + 4L_2 + \frac{4(-1 - 4\ln 3 + 4L_2)}{L_1} + \frac{-28 - 80\ln 3 - 32(\ln 3)^2 - \pi^2 c_1 + 80L_2 + 64(\ln 3)L_2 - 32L_2^2}{L_1^2} + O\left(\frac{L_2^3}{L_1^3}\right)\right]. \tag{26}$$

We solve Eq. (26) for L by iterations and obtain Eq. (11) at the leading order. In that leading-order derivation we neglected the error term $O(\cdots)$ and used Eq. (24). The asymptotic expansion (22) is well convergent for $\beta \lesssim 0.1$ only. It formally limits the applicability of Eq. (11) to $\beta \lesssim 0.1$. For the simulation with the largest shown value, $N/N_c = 1.208$, we have the condition $\beta \gtrsim 0.1$ as seen in Fig. 3, i.e., on the border of Eq. (11) applicability at best. This explains a relatively poor convergence of the numerical simulation value of $L(z)$ to Eq. (11) for $N/N_c = 1.208$ as shown in Fig. 4. We note, however, that even in this case the relative error for $L(z)$ is moderately small: $\lesssim 6\%$. This means that while $N/N_c = 1.208$ is formally beyond the applicability limits of Eq. (11), the numerical error remains moderate and Eq. (11) can be used (with caution) even beyond its formal applicability condition, $\beta \lesssim 0.1$.

IV. EXPERIMENTAL ESTIMATES

In this section we show that the dynamic range of laser intensities for NLSE applicability can be made quite large in experiment to allow the experimental verification of the collapse scaling (11). We identify the required ranges of laser intensity, laser pulse duration, and laser propagation distance in Kerr media for the robust NLSE applicability in the collapse regime. We found above that Eq. (11) is applicable after the initial growth of the pulse amplitude by a factor $\sim$2–3. This implies that the laser intensity increases by a factor $\sim$4–9. For instance, the experimental increase of the laser intensity by 2–3 orders of magnitude would be more than sufficient for the robust identification and verification of the collapse scaling (11). We focus our estimates on the self-focusing of a laser beam in fused silica although our estimates are easy to modify for other Kerr media. We choose for the estimate that $N/N_c = 1.052$ as in the inset of Fig. 1. This determines the collapse distance $z_c \simeq 1.047\,499$ in dimensionless units.

We first consider a stationary self-focusing of the laser beam in Kerr medium. (We assume for now that the pulse duration is long enough to neglect time-dependent effects. We estimate the range of allowed pulse durations below.) The NLSE (1) in dimensional units with added multiphoton absorbtion (MPA) takes the following form (see, e.g., Ref. [35]):

$$i\partial_z\tilde{\psi} + \frac{1}{2k}\nabla^2\tilde{\psi} + \frac{kn_2}{n_0}|\tilde{\psi}|^2\tilde{\psi} + i\frac{\beta^{(K)}}{2}|\tilde{\psi}|^{2K-2}\tilde{\psi} = 0, \tag{27}$$

where $k = 2\pi n_0/\lambda_0$ is the wave number in media, λ_0 is the vacuum wavelength, n_0 is the linear index of refraction, and n_2 is the nonlinear Kerr index. The index of refraction is $n = n_0 + n_2 I$, where $I = |\tilde{\psi}|^2$ is the light intensity. Also K is the number of photons absorbed by the electron in each elementary process (K-photon absorbtion) and $\beta^{(K)}$ is the MPA coefficient. For fused silica with $\lambda_0 = 790$ nm, $n_0 = 1.4535$ and $n_2 = 3.2 \times 10^{-16}$ cm^2/W. A dominated nonlinear absorbtion process for this wavelength is $K = 5$ with $\beta^{(5)} = 1.80 \times 10^{-51}$ cm^7 W^{-4} [35]. The nonlinear Kerr term in Eq. (27) dominates over the MPA term provided the light intensity $I < (\frac{2kn_2}{\beta^{(5)}n_0})^{1/3} \equiv I_{\mathrm{MPA}} \simeq 3 \times 10^{13}$ W/cm^2. The critical power (8) in dimensional units $P_c = \frac{N_c\lambda_0^2}{8\pi^2 n_2 n_0} \simeq 2$ MW.

Assume that we propagate through the fused silica the collimated Gaussian laser beam with the initial intensity distribution $I(\mathbf{r},z=0)=I_{\rm ini}e^{-2r^2/w_0^2}$, where the initial beam waist $w_0=0.5$ cm. The beam power $I_{\rm ini}\pi w_0^2/2$ is just above P_c. Then the initial beam intensity $I_{\rm ini}\simeq 6\times 10^6$ W/cm^2. This means that the dynamic range of the intensities $I_{\rm MPA}/I_{\rm ini}\simeq 5\times 10^6$ of the NLSE applicability is quite large. This estimate for $I_{\rm MPA}$ can be considered as the upper limit of the allowed laser intensity. This limit is valid for ultrashort optical pulse duration (tens of femtoseconds). For longer pulses the MPA eventually results in optical damage. Typical experimental measurements of the optical damage threshold give the threshold intensity $I_{\rm thresh}\sim 5\times 10^{11}$ W/cm^2 for 8-ns pulses and $I_{\rm thresh}\sim 1.5\times 10^{12}$ W/cm^2 for 14-ps pulses [36]. Even these lower estimates give more than 5 orders of the dynamic range of the NLSE applicability. However, for such short pulse durations, t_0, we generally might need to take into account a group velocity dispersion (GVD). Its contribution is described by the addition of the term $-\frac{\beta_2}{2}\frac{\partial^2}{\partial t^2}\tilde{\psi}$ to the left-hand side of Eq. (27). Here $\beta_2=370$ fs^2/cm is the GVD coefficient for $\lambda_0=790$ nm and t is the retarded time $t\equiv T-z/c$, where T is the physical time and c is the speed of light. The collapse distance, $\tilde{z}_c$, in dimensional units is given by $\tilde{z}_c=\frac{4\pi n_0 w_0^2}{\lambda_0}z_c\simeq 600$ m, where we set $z_c\simeq 1.047\,499$ as in the simulation shown in the inset of Fig. 1. At this distance the linear absorbtion of optical grade fused silica is still negligible. The GVD distance $\tilde{z}_{\rm GVD}\equiv 2t_0^2/\beta_2$ must exceed $\tilde{z}_c$ for NLSE applicability, which gives $t_0\gtrsim 3$ ps.

Other possible effects beyond the NLSE include a stimulated Brillouin scattering (can be neglected for the pulse duration $\lesssim$10 ns [37]) and a stimulated Raman scattering (SRS). The threshold of SRS for a long pulse in fused silica was estimated from the gain exponent $gI_0l\simeq 16$, where the peak intensity of the pulse, I_0, was assumed to be constant along the propagation distance, l, and $g\simeq 10^{-11}$ cm/W was the Raman gain constant [37]. This estimate was obtained assuming that the spontaneous emission was amplified by a SRS (with the amplification factor $e^{gI_0l}=e^{16}$) up to the level of the laser pump intensity I_0 [37]. In this paper we modified this SRS threshold estimate to account for the variable pulse intensity along z [the intensity evolves according to Eq. (4)].

The maximum of intensity at $\mathbf{r}=0$ evolves as $I(z)\simeq\frac{L(z_0)^2}{L(z)^2}I_{\rm ini}\simeq\frac{z_c-z_0}{z_c-z}I_{\rm ini}$ for $z>z_0$, where z_0 is defined above ($z_0\simeq 1.0007$ for the simulation of the inset of Fig. 1). Here we assumed for the estimate that the logarithmic contributions to L are slow in z and we replaced them by a constant (compared to the exact expression it gives a $\lesssim$20% difference which is not essential for the rough estimate of the NLSE validity). Also we neglected a small contribution to the total SRS amplification from the range $z<z_0$. The SRS wave intensity I_s is amplified according to $\frac{dI_s(z)}{dz}=gI_s(z)I_{\rm ini}\frac{z_c-z_0}{z_c-z}$ which results in $I_s(z_0+l)=I_s(z_0)\exp\left(gI_{\rm ini}(z_c-z_0)\ln\frac{z_c-z_0}{z_c-z_0-l}\right)$. This means that the collapse replaces the gain exponent $gI_{\rm ini}l$ (of the constant intensity case $I_0=I_{\rm ini}$) by the modified gain exponent $gI_{\rm ini}l\ln\frac{z_c-z_0}{z_c-z_0-l}$, where $l\simeq z_c-z_0$. At the SRS threshold that gain exponent has to be $\simeq$16 as explained above. We now assume that the collapsing filament intensity increases by 6 orders: $\frac{z_c-z_0}{z_c-z_0-l}=10^6$. Then we obtain the gain exponent $gI_{\rm ini}l\ln\frac{z_c-z_0}{z_c-z_0-l}\simeq 2\ll 16$; i.e., we still operate well below the SRS threshold and can neglect the SRS. This SRS threshold estimate is true for relatively long pulses, $\gtrsim$10 ps [37]. For pulses of shorter duration, the SRS is additionally suppressed because the laser beam and the SRS wave move with different group velocities.

We conclude that the optimal pulse duration for the experimental verification of this paper is 3 ps $\lesssim t_0\lesssim$ 10 ns. Note that one can easily reduce the required media length $\tilde{z}_c$ by several orders of magnitude by prefocusing the pulse before it enters the Kerr media. However, the cost of such prefocusing would be a reduction in the dynamic range of the NLSE applicable intensities.

V. NUMERICAL SIMULATIONS OF NLSE

The results presented in this paper are obtained using an adaptive mesh refinement technique [4,38], complemented with the sixth-order Runge-Kutta time advancement method. Some details of that type of technique are provided in Ref. [29]. The spatial derivatives are calculated using an eighth-order finite difference scheme on the nonuniform grid. Our spatial domain, $r\in[0,r_{\rm max}]$, is divided into several subdomains (subgrids) with different spatial resolutions. The spacing between computational points is constant for each subgrid and differs by a factor of 2 between adjacent subgrids. The rightmost subgrid, farthest from the collapse, has the coarsest resolution; the spatial step decreases in the inward direction. The grid structure adapts during the evolution of the collapse to keep the solution well resolved. When a refinement condition is met, the leftmost subgrid is divided in two equal subgrids with the interpolation of up to the tenth order used to initialize the data on the new subgrid. The solution on all subgrids is evolved with the same time step, $\Delta t=C_{\rm CFL}h^2$, where h is the spatial step of the finest grid and $C_{\rm CFL}$ is a constant. Typically we choose $C_{\rm CFL}=0.05$, but we also tested the convergence for smaller values of $C_{\rm CFL}$.

Finally, we comment on how we determine L and β from numerical simulations. At each z we use the following two-step procedure. First, we determine $L(z)$ from the numerical solution $\psi(r,z)$ as $L=\frac{1}{|\psi|}(1+2\frac{|\psi|_{rr}}{|\psi|^3})^{-1/2}|_{r=0}$, an expression derived from the Taylor series expansion of $V_0(\beta,\rho)$ for $\rho\ll 1$ in Eq. (12). Second, we determine $\beta(z)$ from the nonlinear condition $|\psi(0,z)|=\frac{1}{L(z)}V_0(\beta,0)$ using the precomputed values of $V_0(\beta,0)$ from the solution of Eq. (12). We found that this procedure gives much better accuracy in determining L and β than the alternative procedures reviewed, e.g., in Ref. [16].

VI. CONCLUSION

In conclusion, we found that the collapsing solution is described by the approximate self-similar solution $|\psi(r,z)|=\frac{1}{L(z)}V_0(\beta(z),\frac{r}{L(z)})$ for $0\leqslant r/L(z)\lesssim 2/\beta^{1/2}(z)$, with $L(z)$ given by Eq. (11) and $\beta=-L^3L_{zz}$, where $V_0(\beta,\rho)$ is the ground-state soliton solution of Eq. (12). The slow dependence of β on z results in adiabatically slow violation of self-similarity. For $r/L(z)\gg 2/\beta^{1/2}(z)$ the collapsing solution has the tail $\tilde{V}_0$ from Eq. (13). We found that the dependence of $L(z)$ in Eq. (11) is in very good agreement with the direct numerical

simulations, as shown in Fig. 1, starting from quite moderate increase (∼2–3 times) of the amplitude of the initial Gaussian beam. By the direct substitution of the values $L(z_0)$ and $\beta(z_0)$ into Eq. (11), with z_0 defined in Fig. 1, one can see that expression (11) matches the classical result, Eq. (9), with accuracy of ∼10–20% only for the unrealistically large amplitudes given by Eq. (10). This suggests that the classical result, Eq. (9), while being asymptotically correct, should be replaced by the much more accurate new formula, Eq. (11), for any currently foreseeable physical systems.

ACKNOWLEDGMENTS

This work was supported by the National Science Foundation under Grants No. DMS 0807131, No. PHY 1004118, and No. PHY 1004110.

[1] G. A. Askar'yan, Sov. Phys. JETP-USSR **15**, 1088 (1962).
[2] R. Y. Chiao, I. Garmire, and C. H. Townes, Phys. Rev. Lett. **13**, 479 (1964).
[3] R. W. Boyd, *Nonlinear Optics* (Elsevier, Boston, 2008).
[4] C. Sulem and P. L. Sulem, *Nonlinear Schrödinger Equations: Self-Focusing and Wave Collapse* (World Scientific, New York, 1999).
[5] L. P. Pitaevskii and S. Stringari, *Bose-Einstein Condensation* (Clarendon, Oxford, 2003).
[6] V. E. Zakharov and A. B. Shabat, Sov. Phys. JETP-USSR **34**, 62 (1972).
[7] S. N. Vlasov, V. A. Petrishchev, and V. I. Talanov, Izv. Vyssh. Uchebn. Zaved., Radiofiz. **14**, 1353 (1971).
[8] V. E. Zakharov, Sov. Phys. JETP-USSR **35**, 908 (1972).
[9] P. M. Lushnikov and H. A. Rose, Phys. Rev. Lett. **92**, 255003 (2004).
[10] P. M. Lushnikov and H. A. Rose, Plasma Phys. Controlled Fusion **48**, 1501 (2006).
[11] L. Bergé, S. Skupin, F. Lederer, G. Méjean, J. Yu, J. Kasparian, E. Salmon, J. P. Wolf, M. Rodriguez, L. Wöste *et al.*, Phys. Rev. Lett. **92**, 225002 (2004).
[12] S. Dyachenko, A. C. Newell, A. Pushkarev, and V. E. Zakharov, Phys. D **57**, 96 (1992).
[13] P. M. Lushnikov and N. Vladimirova, Opt. Lett. **35**, 1965 (2010).
[14] V. I. Talanov, JETP Lett. **11**, 199 (1970).
[15] E. A. Kuznetsov and S. K. Turitsyn, Phys. Lett. A **112**, 273 (1985).
[16] G. Fibich and G. Papanicolaou, SIAM J. Appl. Math. **60**, 183 (1999).
[17] V. M. Malkin, Phys. D **64**, 251 (1993).
[18] G. M. Fraiman, Sov. Phys. JETP-USSR **61**, 228 (1985).
[19] B. J. LeMesurier, G. Papanicolaou, C. Sulem, and P. L. Sulem, Phys. D **31**, 78 (1988).
[20] V. M. Malkin, Phys. Lett. A **151**, 285 (1990).
[21] F. Merle and P. Raphael, J. Am. Math Soc. **19**, 37 (2006).
[22] N. E. Kosmatov, V. F. Shvets, and V. E. Zakharov, Phys. D **52**, 16 (1991).
[23] G. D. Akrivis, V. A. Dougalis, O. A. Karakashian, and W. R. McKinney, SIAM J. Sci. Comput. **25**, 186 (2003).
[24] M. A. Herrero and J. J. L. Velázquez, Math. Ann. **306**, 583 (1996).
[25] J. J. L. Velazquez, SIAM J. Appl. Math. **62**, 1581 (2002).
[26] P. M. Lushnikov, Phys. Lett. A **374**, 1678 (2010).
[27] S. I. Dejak, P. M. Lushnikov, Y. N. Ovchinnikov, and I. M. Sigal, Phys. D **241**, 1245 (2012).
[28] S. A. Dyachenko, P. M. Lushnikov, and N. Vladimirova, AIP Conf. Proc. **1389**, 709 (2011).
[29] S. A. Dyachenko, P. M. Lushnikov, and N. Vladimirova, arXiv:1301.5604 [Nonlinearity (to be published)].
[30] L. D. Landau and L. M. Lifshitz, *Quantum Mechanics Non-Relativistic Theory,* Vol. 3, 3rd ed. (Butterworth-Heinemann, Oxford, 1981).
[31] L. Bergé and D. Pesme, Phys. Lett. A **166**, 116 (1992).
[32] L. Bergé, Phys. Rep. **303**, 259 (1998).
[33] Y. V. Sidorov, M. V. Fedoryuk, and M. I. Shabunin, *Lectures on the Theory of Functions of a Complex Variable* (Mir Publishers, Moscow, 1985).
[34] F. W. J. Olver, *Asymptotics and Special Functions* (Academic Press, New York, 1974).
[35] L. Bergé, S. Skupin, R. Nuter, J. Kasparian, and J.-P. Wolf, Rep. Prog. Phys. **70**, 1633 (2007).
[36] A. V. Smith and B. T. Do, Appl. Opt. **47**, 4812 (2008).
[37] G. Agrawal, *Nonlinear Fiber Optics*, 5th ed. (Academic Press, Oxford, 2012).
[38] M. J. Berger and P. Colella, J. Comput. Phys. **82**, 64 (1989).